European Journal of Nuclear Medicine and Molecular Imaging (2019) 46:2270–2279
https://doi.org/10.1007/s00259-019-04427-z

ORIGINAL ARTICLE

Personalised radioembolization improves outcomes in refractory intra-hepatic cholangiocarcinoma: a multicenter study

Hugo Levillain[1] · Ivan Duran Derijckere[1] · Lieveke Ameye[2] · Thomas Guiot[3] · Arthur Braat[4] · Carsten Meyer[5] · Bruno Vanderlinden[3] · Nick Reynaert[3] · Alain Hendlisz[6] · Marnix Lam[4] · Christophe M. Deroose[7] · Hojjat Ahmadzadehfar[8] · Patrick Flamen[1]

Received: 5 April 2019 / Accepted: 3 July 2019 / Published online: 19 July 2019

Abstract

Purpose Reported outcomes of patients with intra-hepatic cholangiocarcinoma (IH-CCA) treated with radioembolization are highly variable, which indicates differences in included patients' characteristics and/or procedure-related variables. This study aimed to identify patient- and treatment-related variables predictive for radioembolization outcome.

Methods This retrospective multicenter study enrolled 58 patients with unresectable and chemorefractory IH-CCA treated with resin ^{90}Y-microspheres. Clinicopathologic data were collected from patient records. Metabolic parameters of liver tumor(s) and presence of lymph node metastasis were measured on baseline ^{18}F-FDG-PET/CT. ^{99m}Tc-MAA tumor to liver uptake ratio (TLR_{MAA}) was computed for each lesion on the SPECT-CT. Activity prescription using body-surface-area (BSA) or more personalized partition-model was recorded. The study endpoint was overall survival (OS) starting from date of radioembolization. Statistical analysis was performed by the log-rank test and multivariate Cox's proportional hazards model.

Results Median OS (mOS) post-radioembolization of the entire cohort was 10.3 months. Variables associated with significant differences in terms of OS were serum albumin (hazard ratio (HR) = 2.78, 95%CI:1.29–5.98, $p = 0.002$), total bilirubin (HR = 2.17, 95%CI:1.14–4.12, $p = 0.009$), aspartate aminotransferase (HR = 2.96, 95%CI:1.50–5.84, $p < 0.001$), alanine aminotransferase (HR = 2.02, 95%CI:1.05–3.90, $p = 0.01$) and γ-GT (HR = 2.61, 95%CI:1.31–5.22, $p < 0.001$). The presence of lymph node metastasis as well as a $TLR_{MAA} < 1.9$ were associated with shorter mOS: HR = 2.35, 95%CI:1.08–5.11, $p = 0.008$ and HR = 2.92, 95%CI:1.01–8.44, $p = 0.009$, respectively. Finally, mOS was significantly shorter in patients treated according to the BSA method compared to the partition-model: mOS of 5.5 vs 14.9 months (HR = 2.52, 95%CI:1.23–5.16, $p < 0.001$). Multivariate analysis indicated that the only variable that increased outcome prediction above the clinical variables was the activity prescription method with HR of 2.26 (95%CI:1.09–4.70, $p = 0.03$). The average mean radiation dose to tumors was significantly higher with the partition-model (86Gy) versus BSA (38Gy).

Conclusion Radioembolization efficacy in patients with unresectable recurrent and/or chemorefractory IH-CCA strongly depends on the tumor radiation dose. Personalized activity prescription should be performed.

Keywords Intra-hepatic cholangiocarcinoma · Radioembolization · SIRT · Yttrium-90 · Resin microspheres

Introduction

Intra-hepatic cholangiocarcinoma (IH-CCA) is a rare malignancy of the biliary epithelium arising in the biliary ducts within the liver parenchyma and is the second most common primary hepatic malignancy after hepatocellular carcinoma worldwide [1]. Prognosis is poor with median survival estimated between 3 and 8 months when left untreated [2–4]. Surgery and liver transplantation are the only curative approaches; nevertheless, they are not always feasible as most patients are diagnosed at an advanced stage of the disease

This article is part of the Topical Collection on Oncology - Digestive Tract.

Electronic supplementary material The online version of this article (https://doi.org/10.1007/s00259-019-04427-z) contains supplementary material, which is available to authorized users.

✉ Hugo Levillain
hugo.levillain@bordet.be

Extended author information available on the last page of the article

given its clinically silent course [5]. Several non-curative therapies have been attempted to improve survival in unresectable IH-CCAs. Currently, cisplatin-gemcitabine is the standard of care following the results of the ABC-02 study which had relatively poor results with a median overall survival (mOS) of 11.7 months [6]. In non-resectable disease limited to the liver locoregional ablative treatments have been proposed. Among them, radioembolization with ^{90}yttrium-labelled resin or glass microspheres seems attractive because most tumours in the liver have a high arterial perfusion. However, reported efficacies in recurrent and/or chemorefractory patients have been highly variable with mOS ranging from 7 to 22 months suggesting wide variation in included patients' characteristics and/or procedure-related variables [7–10]. This study aimed to identify patient and treatment-related variables predictive of radioembolization outcome.

Materials and methods

Study design and patient selection

This retrospective multicentre study enrolled 58 patients with intrahepatic cholangiocarcinoma (IH-CCA) treated between January 2004 and September 2018 with resin ^{90}Y-microsphere (SIR-Spheres, Sirtex medical Ltd., Sydney, Australia) in four European radioembolization expert centres. Inclusion criteria were: 18 years of age or older, histologically confirmed IH-CCA, unresectable at initial diagnosis or recurrence after primary surgery, liver-only or liver predominant disease, refractory to one or more lines of chemotherapy, peformance status <2, and adequate liver function without ascites. Exclusion criteria were: prior radioembolization or external beam radiotherapy, chemotherapy within the last 4 weeks prior to radioembolization, second active cancer and predominant extra-hepatic disease. This study was approved by the Jules Bordet Institute Ethics Committee (CE2575) and Ethics Committees of all other participating centres. For this retrospective study formal consent was not required.

Clinical and biological data

The clinicopathologic data of the 58 patients included in the study were collected from the patients' records. These data included the demographic characteristics, biological and pathological features of the tumour, time between initial diagnosis and radioembolization, liver surgery and the number of previous chemotherapy lines. Notably, tumour burden (uni or multifocal) and tumour distribution (uni or bilobar) information were extracted from medical files and were determined from anatomic and/or metabolic images independently of tumour size.

^{18}F-FDG-PET/CT and ^{99m}Tc-MAA-SPECT/CT imaging procedures

Thirty-seven patients had a ^{18}F-FDG-PET/CT prior to radioembolization. All ^{18}F-FDG-PET/CT images were acquired with EARL-approved settings to guarantee image quality standardisation. PET/CT systems involved were Siemens Biograph 2, General Electric Discovery 690 time-of-flight (TOF), Siemens Biograph mCT TOF and Siemens Biograph TruePoint. Patients were required to have fasted for at least 6 h and to have blood glucose levels <150 mg/dL before ^{18}F-FDG injection. Images were acquired 60 min after injection (range: 60–70 min) of 4 MBq/kg (range: 2.6–5.4 MBq/kg). Attenuation and scatter corrections were applied on all images.

Forty-four patients had a pre-treatment SPECT/CT after intra-arterial injection of labeled macro-aggregated albumin (^{99m}Tc-MAA). SPECT/CT systems involved were Siemens Symbia T2, T and T16. Images were acquired 60 min after injection (range: 30–120 min) of 206 MBq (range: 80–340 MBq) of ^{99m}Tc-MAA. Attenuation and scatter corrections were applied on all images.

After local de-identification, all ^{18}F-FDG-PET/CT and ^{99m}Tc-MAA-SPECT/CT images were transferred and centralised at the Imaging Core Lab of Institut Jules Bordet.

^{18}F-FDG-PET/CT analysis

All ^{18}F-FDG-PET/CT images were analyzed using dedicated commercial software (PET VCAR v.4.6®; Advantage Workstation; GE Healthcare).

Criteria for identification of target lesions and delineation process

Criteria for identification of target lesions were adapted from PERCIST 1.0 [10]. ^{18}F-FDG-PET/CT measurable target lesions were defined as follows: lesion size >2 cm in longest axial diameter and ^{18}F-FDG uptake with standard uptake value (SUV) normalized to lean body mass > 1.5 × mean liver SUV (SUV_{mean}(non-tumoural-liver)) + 2 standard deviations of liver SUV (SD(non-tumoural-liver)). Non-tumoural-liver (NTL) background ^{18}F-FDG uptake was determined by drawing a reference volume as a 3-cm diameter spherical volume of interest (VOI) located in the healthy liver parenchyma. Lesions were delineated using a fixed threshold corresponding to the PERCIST criteria: 1.5 × SUV_{mean} (NTL) + 2SD(NTL). Therefore, necrotic parts of tumour were not included in the VOI. ^{18}F-FDG uptake bridging between two or more lesions was manually corrected. The maximal number of target lesions was not restricted and all delineations were validated by an experienced nuclear medicine physician blinded to the clinical and outcome data of the patients.

Baseline metabolic parameter assessment

SUV_{mean}(NTL) was measured for each patient. Metabolic parameters of interest, measured for each delineated target lesion, were: metabolic tumour volume (MTV), SUV_{max}, SUV_{peak}, SUV_{mean}, total lesion glycolysis (TLG) and tumour to NTL uptake ratio (TLR), defined as the tumour SUV_{peak} divided by the SUV_{mean}(NTL). When multiple hepatic lesions were present, the metabolic value retained to characterise the patient evolution was the highest value among the lesions. The total metabolic tumour volume (TMTV) corresponding to the sum of the MTV of all delineated lesions was finally computed for each patient.

Planning and administration of ^{90}Y-microspheres

Workup and treatment were performed following the local standard of practice and according to the manufacturer's recommendations. Activity prescription of ^{90}Y-microspheres was performed using either the body surface area (BSA) or partition-model. Briefly, the BSA method determines the activity of ^{90}Y-microspheres to administer by computing the patient's body surface area, assumed to correlate with the patient's liver volume [11]. And the partition-model computes the maximal activity that can be administered based on tumour to non-tumoural liver uptake ratio (assessed on ^{99m}Tc-MAA_SPECT/CT) and on patient specific liver, lungs and tumour mass, while maintaining a safe dose (≤40Gy) for non-treated liver and (≤20Gy) lungs [12]. Tumour dose evaluation was performed using only the volume of viable tumour, excluding necrosis.

The administered ^{90}Y-microspheres activity was collected for each patient from the medical record.

Pre-treatment ^{99m}Tc-MAA-SPECT/CT analysis

All ^{99m}Tc-MAA-SPECT/CT images were analyzed using dedicated commercial software (Planet Onco 3.0®; Dosisoft).

Determination of the administered ^{90}Y-microspheres volumic activity

For each of the 44 patients presenting a ^{99m}Tc-MAA–SPECT/CT, the whole liver volume was determined by manual delineation on CT images. In case of lobar or segmental treatment an additional delineation of the treated liver was performed on ^{99m}Tc-MAA-SPECT images using a semi-automatic method based on a threshold. For each patient the threshold value was adjusted so that the isocontour of the ^{99m}Tc-MAA distribution volume visually fits best with anatomic images. The administered ^{90}Y-microspheres volumic activity ($A_{vol}(^{90}Y)$) was computed for the 44 patients by dividing the administered ^{90}Y-microspheres activity by the treated liver volume.

Pre-treatment ^{99m}Tc-MAA uptake

From the 58 patients included in this study, 23 had a complete image set containing both baseline ^{18}F-FDG-PET/CT and ^{99m}Tc-MAA-SPECT/CT. Lesions delineated on baseline ^{18}F-FDG-PET/CT were projected on the liver-based anatomically registered ^{99m}Tc-MAA-SPECT/CT, using rigid registration method. The lesions VOI were morphologically subtracted from the whole liver VOI to obtain the NTL VOI. Then ^{99m}Tc-MAA lesion uptake to NTL uptake ratio (TLR_{MAA}) was computed for each lesion by dividing the number of counts within the lesion by the number of counts within the NTL. When multiple hepatic lesions were present, the TLR_{MAA} value retained to characterise the patient was the lowest value among the lesions.

Pre-treatment ^{99m}Tc-MAA dosimetry

The pre-treatment time-integrated activity map for ^{90}Y-microspheres was derived from the ^{99m}Tc-MAA-SPECT/CT dataset, assuming similar distributions within the treated liver for ^{90}Y-microspheres and ^{99m}Tc-MAA. Voxel-based 3D dosimetry was performed by convolving the time-integrated activity map with Voxel-S-value as described by Dieudonne et al. [13]. The dose volume histogram was computed for all target lesions and the NTL of the 23 patients that had a complete image set. Finally, corresponding mean absorbed doses (NTL-D_{mean} and lesion-D_{mean}) were determined.

Statistical method

Descriptive analyses were performed to summarise baseline patient characteristics and ^{90}Y-microsphere treatment. The Kaplan-Meier product limit method was used to describe OS curves. OS was defined as the time between radioembolization and death or last follow-up (date of censoring). Univariate associations between the explanatory variables and the outcome OS were examined by the log rank test. Continuous variables were dichotomized by using their respective median as cut-off value. A correlation matrix was computed for all continuous variables in order to identify highly correlated parameters (Spearman's correlation ≥0.8) and to investigate a possible problem of multicollinearity in multivariate analysis. Variables with $p < 0.05$ by univariate analysis and low intercorrelation were included in multivariate analysis. Multivariate Cox's proportional hazards model was performed for selected combinations of predictive factors to determine the independent predictive significance of each combination. As the considered variables are not available in all patients (only 10 cases with complete data for all variables, e.g. ^{18}F-FDG-PET/CT was not performed in all patients), the

variable selection was performed in several steps in order to respect the rule of thumb of ten events per predictor. First we considered biology variables available in the majority of the patients as explanatory variables (i.e. fixed variables) and computed a predictive score for OS (PS_{OS}) using their parameter estimates as weights. Then, the remaining variables were added one by one to the score in order to identify variables that improve the hazard ratio of the model already containing the score. Finally, differences between patients treated by BSA method and patients treated with partition-model were investigated. All continuous variables within the two groups were checked for normality, using the D'Agostino and Pearson normality test, and described with conventional statistics. Differences in demographic, clinical, pathological and treatment data were compared using t-test or Mann-Whitney test for continuous variables and χ^2 (Fisher's exact) test for discrete variables. The statistical analyses were performed using the GraphPad® software (version 7.4; Prism, La Jolla California, USA) except for the multivariate analysis which was performed with SAS® software (version 9.4; SAS Institute Inc., Cary, NC, USA).

Results

Patients baseline characteristics

The 58 patients included in this study had a median age of 66 years (range 40–88 years) and the median duration from primary diagnostic to radioembolization was 9 months (range 3–42 months). All patients underwent surgery and/or chemotherapy. Baseline characteristics are presented in Table 1.

Table 1 Baseline characteristics of patients

Characteristic	Number of patients	Value, *n* (%) or median (range)
Sex	58	
Male		23 (40%)
Female		35 (60%)
Age (y)	58	66 (40–88)
BMI (kg/m^2)	58	25 (19–37)
Time between diagnosis and radioembolization (months)	58	9 (3–42)
Biological		
Haemoglobin (g/dl)	50	11.5 (7.8–16.6)
Albumin (g/dl)	37	3.9 (2.7–4.7)
Prothrombin time (%)	50	92 (60–135)
Total Bilirubin (mg/dl)	50	0.53 (0.18–1.9)
Aspartate aminotransferase (UI/L)	50	33 (14–146)
Alanine aminotransferase (UI/L)	50	28 (9–90)
Alkaline phosphatase (UI/L)	35	241 (58–2015)
γ-GT (UI/L)	50	205 (20–1542)
Lactate dehydrogenase (UI/L)	43	326 (149–641)
Liver surgery	58	
Yes		30 (52%)
No		28 (48%)
Number of chemotherapy lines before radioembolization	58	
< 2		43 (74%)
≥ 2		15 (26%)
Tumour burden	58	
Solitary		27 (47%)
Multifocal		31 (53%)
Tumour distribution	58	
Unilobar		25 (43%)
Bilobar		33 (57%)
Activity prescription method	58	
BSA		27 (47%)
Partition-model		31(53%)

Baseline ^{18}F-FDG-PET/CT and pre-treatment ^{99m}Tc-MAA-SPECT/CT analysis

Among the 37 patients who had a baseline ^{18}F-FDG-PET/CT, 80 lesions were delineated out of which 25 had to be excluded from analysis (diameter < 2 cm), resulting in 55 evaluable lesions. All 37 patients had at least one evaluable lesion. Among the 23 patients that had a complete imaging set, 32 lesions were evaluable. The median patient-based TLR_{MAA} was 1.9 (range 0.5–5.1). Baseline ^{18}F-FDG-PET/CT and ^{99m}Tc-MAA-SPECT/CT analysis are presented in Supplementary material 1.

Survival

The median follow-up for all patients after radioembolization was 6.3 months. The Kaplan-Meier survival estimate for the entire cohort of 58 patients is presented on Fig. 1. Among the 58 patients, 12 were censored because of endpoint not reached at last follow-up. The mOS post- radioembolization was 10.3 months. The 1- and 2-year survival rates after radioembolization were 40% and 22%, respectively.

Univariate analysis

Table 2 summarises the median survivals of the dichotomised baseline characteristics. Several biological parameters were associated with significant differences in terms of OS. The mOS was significantly shorter in patients with hypermetabolic lymph nodes on ^{18}F-FDG-PET/CT compared to patients without hypermetabolic lymph nodes (mOS 7.1 versus 14.9 months; HR 2.35 (95% CI 1.08–5.11), $p = 0.008$), as well as for patients with $TLR_{MAA} < 1.9$ compared to patients with

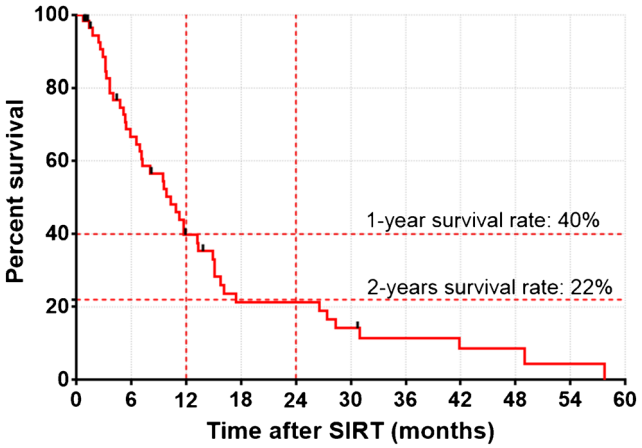

Fig. 1 Overall survival estimated by the Kaplan-Meier method for the entire cohort

$TLR_{MAA} \geq 1.9$ (mOS 9.4 versus 16.2 months; HR 2.92 (95% CI 1.01–8.44), $p = 0.009$). The mOS was significantly shorter in patients treated according to the standard BSA method compared to patients treated according to partition-model (mOS 5.5 versus 14.9 months; HR 2.52 (95%CI 1.23–5.16), $p = <0.001$). Figure 2 shows the OS curves.

Continuous variables correlation

Supplementary material 2 shows the correlation matrix. Out of total 20 variables analysed only the seven metabolic values derived from baseline ^{18}F-FDG-PET/CT images presented a high correlation (Spearman's correlation ≥0.8). All variables identified as predictive factors of OS in the univariate analysis did not show high intercorrelation.

Table 2 Univariate analysis of predictive factors for overall survival in patient with IH-CCA

Variables	Dichotomisation	Overall survival			
		Median (months)	Hazard ratio (HR)	95%CI	*p*-value
Sex	Female vs male	9.8 vs 10.3	1.21	0.65–2.25	0.53
Age (y)	≥ 66 vs < 66	9.9 vs 10.2	1.04	0.56–1.97	0.91
BMI (kg/m^2)	≥ 25 vs < 25	9.9 vs 10.9	1.42	0.67–2.90	0.28
Time between diagnostic and treatment (months)	≥ 8.6 vs < 8.6	9.8 vs 10.3	1.17	0.57–2.13	0.73
Haemoglobin (g/dl)	< 11.5 vs ≥ 11.5	7.2 vs 11.7	1.35	0.72–2.53	0.33
Albumin (g/dl)	< 3.9 vs ≥ 3.9	6.6 vs 15.1	2.78	1.29–5.98	**0.002**
Prothrombin time (%)	< 92 vs ≥ 92	6.2 vs 11.7	1.37	0.73–2.55	0.31
Total Bilirubin (mg/dl)	≥ 0.53 vs < 0.53	7.2 vs 14.9	2.17	1.14–4.12	**0.009**
Aspartate aminotransferase (UI/L)	≥ 33 vs < 33	5.9 vs 15.1	2.96	1.50–5.84	**<0.001**
Alanine aminotransferase (UI/L)	≥ 28 vs < 28	9.4 vs 12.5	2.02	1.05–3.9	**0.01**
Alkaline phosphatase (UI/L)	≥ 241 vs < 241	7.2 vs 13.3	1.73	0.81–3.69	0.13
γ-GT (UI/L)	≥ 205 vs < 205	5.2 vs 15.1	2.61	1.31–5.22	**<0.001**
Lactate dehydrogenase (UI/L)	≥ 326 vs < 326	6.9 vs 10.3	1.02	0.53–1.98	0.94
Liver surgery	No vs Yes	8.1 vs 11.3	1.23	0.68–2.21	0.5
Number of chemotherapy lines before radioembolization	≥ 2 vs <2	8.6 vs 10.1	1.75	0.76–2.39	0.16
Tumour burden	Multifocal vs solitary	9.8 vs14.9	1.79	0.74–4.29	0.31
Tumour distribution	Bilobar vs unilobar	6.6 vs 11.7	1.53	0.81–2.88	0.13
Hypermetabolic lymph nodes	Presence vs absence	7.1 vs 14.9	2.35	1.08–5.11	**0.008**
TMTV (ml)	≥ 106 vs < 106	11 vs 12.3	1.47	0.67–3.21	0.3
SUV_{max} (g/ml)	≥ 9 vs < 9	10.3 vs 14.9	1.67	0.75–3.69	0.17
SUV_{peak} (g/ml)	≥ 7 vs < 7	10.3 vs 14.9	1.8	0.81–4.01	0.16
SUV_{mean} (g/ml)	≥ 4 vs < 4	11 vs 12.3	1.3	0.60–2.81	0.5
MTV (ml)	≥ 57 vs < 57	11.8 vs 10.8	1.27	0.58–2.75	0.53
TLG (g)	≥ 249 vs < 249	11.8 vs 10.8	1.27	0.58–2.75	0.53
TLR	≥ 4 vs < 4	10.3 vs 13.3	1.64	0.68–3.93	0.22
TLR_{MAA}	< 1.9 vs ≥ 1.9	9.4 vs 16.2	2.92	1.01–8.44	**0.009**
Activity prescription method	BSA vs partition-model	5.5 vs 14.9	2.52	1.23–5.16	**<0.001**

p-values presented in bold text were considered significant

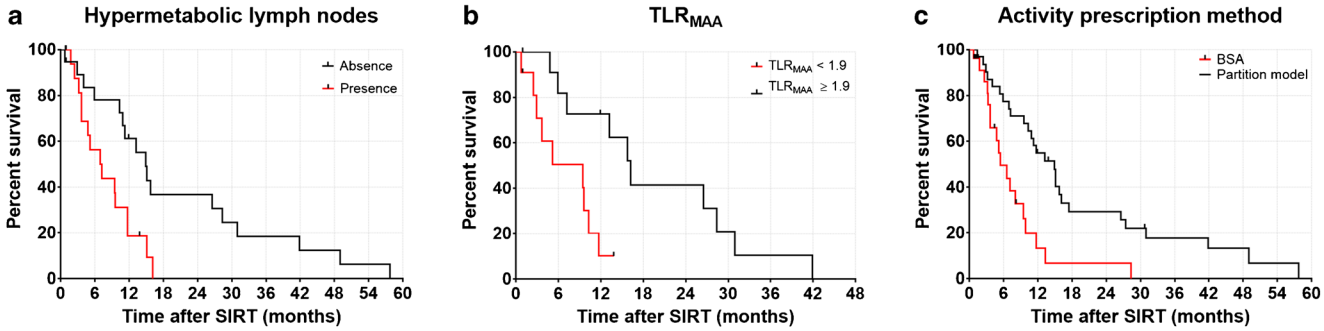

Fig. 2 OS curves estimated by the Kaplan-Meier method stratified by (*A*) absence or presence of hypermetabolic lymph nodes, (*B*) TLR_{MAA}, (*C*) the activity prescription method (BSA vs partition-model)

Multivariate analysis

Results of the multivariate Cox's proportional hazards model analysis for the explanatory variables: total bilirubin, Aspartate aminotransferase, Alanine aminotransferase and γ-GT (biological parameters available in the majority of patients) are presented in Table 3. The Alanine aminotransferase was not retained by the model.

The predictive score of the model was defined as follows: PSos = 0.7× (1 if total bilirubin>0.53 mg/dl) + 1.0 × (1 if Aspartate aminotransferase>33 UI/L) + 0.9× (1 if γ-GT >205 UI/L). The minimum value of the score is 0 when the values of a patient are lower than the median for total bilirubin, aspartate aminotransferase and γ-GT. The maximum value is 2.6, when the values of a patient are higher than the median for total bilirubin, aspartate aminotransferase and γ-GT. Hazard ratio increase by 2.83 (1.85 to 4.33, $p < 0.001$) per one-unit in the score. The PSos, defined by multivariate analysis, was then used to assess the added predictive value of the remaining variables.

Table 4 shows the results of the multivariate Cox's proportional hazards model analysis for the remaining variables when added one by one to the model. The albumin, alkaline phosphatase, hypermetabolic lymph nodes detected on baseline ^{18}F-FDG-PET/CT and TLR_{MAA} did not improve the model already containing PS_{OS}. However, the activity prescription method (BSA vs partition-model) does significantly improve the model containing PS_{OS}, with a HR for BSA compared to the partition-model of 2.26 (95%CI 1.09–4.70, $p = 0.03$).

Difference in patient treated by BSA or partition-model methods

Comparison between patients treated with the BSA method and patients treated with the partition-model are presented in Supplementary material 3. No difference in terms of demographic, clinicopathologic or ^{18}F-FDG-PET/CT image-derived parameters were observed between patients treated according to BSA method and partition-model for ^{90}Y-microspheres activity prescription. Interestingly, tumour burden ($p = 0.18$), tumour distribution ($p = 0.85$), TLR_{MAA} ($p = 0.20$) and NTL-D_{mean} ($p = 0.16$) were similar in both patient subsets. Significant statistical differences were found between BSA and partition-model cohorts only for $A_{vol}(^{90}Y)$ (BSA group: 19 patients, partition-model group: 25 patients) and lesion-D_{mean} (BSA group: 13 lesions, partition-model group: 19 lesions), that were 1.9-fold and 2.3-fold greater, respectively, in the partition-model group than in the BSA group: median-value of 1.4 MBq/ml (Q1 = 0.84 MBq/ml, Q3 = 2.2 MBq/ml) vs 0.98 MBq/ml (Q1 = 0.69 MBq/ml, Q3 = 1.2 MBq/ml), $p = 0.023$ and median-value of 84 Gy (Q1 = 50 Gy, Q3 = 110 Gy) vs 41 Gy (Q1 = 23.75 Gy, Q3 = 75 Gy), $p < 0.001$, respectively.

Table 3 Multivariate Cox's proportional hazard model for creation of PS_{OS}

Parameter	Number of measures	Parameter estimate	Hazard ratio (HR)	95% CI	*p*-value
Total bilirubin (≥ 0.53 vs < 0.53)	50	0.7	2.09	1.07–4.07	**0.03**
Aspartate aminotransferase (≥ 33 vs < 33)	50	1.0	2.82	1.35–5.90	**0.006**
Alanine aminotransferase (≥ 28 vs < 28)	50	– 0.1	0.89	0.39–2.02	0.78
γ-GT (≥ 205 vs < 205)	50	0.9	2.54	1.21–5.34	**0.01**

p-values presented in bold text were considered significant

Table 4 Multivariate Cox's proportional hazard model for assessing the ability of the remaining variables to improve PS_{OS}

Parameter added to the model	Number of measures	Hazard ratio (HR)	95% CI	*p*-value
Albumin (< 3.9 vs ≥ 3.9)	37	1.51	0.64–3.57	0.34
Alkaline phosphatase (≥ 241 vs < 241)	35	1.65	1.72–3.80	0.24
Hypermetabolic lymph nodes (presence vs absence)	37	1.88	0.76–4.61	0.17
TLR_{MAA} (<1.9 vs ≥ 1.9)	23	1.56	0.32–7.69	0.58
Activity prescription method (BSA vs partition-model)	58	2.26	1.09–4.70	**0.03**

p-values presented in bold text were considered significant

Discussion

This multicenter retrospective study identified patient and treatment-related variables predictive of outcome in a large cohort of patients with unresectable recurrent and/or chemorefractory IH-CCA treated with radioembolization in four European radioembolization reference centers. Our results demonstrated that, beyond classical clinical parameters, the method used for ^{90}Y-microspheres activity prescription was the only independent predictor of outcome after radioembolization. Using the partition model versus the BSA method was associated with a significantly higher estimated tumour absorbed radiation dose (86Gy vs 38Gy; $p < 0.001$) which resulted in a significant improvement of mOS (14.9 vs 5.5 months; HR 0.44, $p < 0.001$). This finding is in line with other studies that demonstrated a dose–response relationship of radioembolization in other tumour types such as colorectal liver metastases and HCC [14–16].

This is, to the best of our knowledge, the first study that identifies significant outcome differences between the BSA method and the more personalized partition-model. Both methods are standard methods for activity prescription of resin microsphere radioembolization, as notified in the official package insert of the device [17]. Currently, most centers use the BSA method because of its simplicity and extensive documentation of its safety. Additionally, a more conservative variant of the BSA method, resulting in lower prescribed activities compared to the classical BSA method, was used in SIRFLOX and FOXFIRE trials. These trials showed negative results when radioembolization was combined with chemotherapy in first line treatment of liver metastatic CRC [18–20].

The BSA method determines the prescribed activity of ^{90}Y-microspheres by computing the patient's body surface area, assumed to correlate with the patient's liver volume, adjusted with the percentage of tumour involvement and magnitude of the lung shunt fraction. However, it has been shown that the patient's body surface area is only moderately correlated to liver volume and that the percentage of tumour involvement has little added value for the adjustment of the activity to administer [11]. On the other hand, the partition-model method is more sophisticated and relies on the Medical Internal Radiation Dose formalism [12]. It separates the lungs, liver and tumours into different compartments and computes the maximal activity that can be administered, while maintaining a safe dose for non-treated liver (≤40Gy) and lungs (≤20Gy). These absorbed dose safety limits were derived from external beam radiotherapy dose limits for liver and lungs homogeneous irradiation based on biological effective doses [21]. The partition-model also takes into account the tumour to non-tumoural liver uptake ratio, assessed on ^{99m}Tc-MAA SPECT/CT images, e.g. when a very targeted focal uptake is observed, higher activity could be administered. Furthermore, this model incorporates the patient specific liver and tumour masses as assessed by anatomic and metabolic image delineation and is therefore recognized as a more personalised and accurate method to determine the activity to administer [22]. The partition-model, compared to the BSA method, requests additional resources: multimodality 3D delineation, ^{99m}Tc-MAA SPECT/CT images acquisition and a medical physicist expert. Nevertheless, radioembolization dedicated treatment planning and post-treatment evaluation software are now getting more widely available, which facilitates its implementation in clinical routine.

Importantly, in our study cohort we did not identify any significant biases in the choice between patients treated according to the BSA method and the partition-model for ^{90}Y-microspheres activity prescription: tumour burden ($p = 0.18$), tumour distribution ($p = 0.85$) and TLR_{MAA} ($p = 0.20$) were similar in both patient subsets, indicating that the choice between the two methods was only based on local preferences and expertise and not on patient characteristics. Besides, demographic parameters, liver surgery and number of chemotherapy lines before radioembolization, tumour burden and tumour distribution were not correlated with OS, which was similarly observed in previous studies [7, 8].

In patients treated according to both partition-model and BSA method, patient's average NTL-D_{mean} were lower than the cut-off value of 40Gy for hepatic toxicity, which confirms that the partition-model method provides an optimized activity to administer by maximising the dose to the lesion while remaining safe for organs at risks.

The univariate analyses indicated two other significant variables predictive of outcome: presence of hypermetabolic lymph node metastasis on ^{18}F-FDG-PET/CT, and the ^{99m}Tc-MAA tumor to non-tumoral-liver uptake ratio. ^{18}F-FDG-PET/CT is a well-established metabolic imaging in oncology for assessment of initial extension, therapy response and has been proven to have a prognostic value in various tumour types [23–25]. In our study, only the presence of hypermetabolic lymph node metastasis was significantly associated with a reduced OS in univariate analysis.

^{99m}Tc-MAA uptake serves as a surrogate measurement for tumours' arterial vascularisation. Thelen et al. demonstrated that tumour-associated angiogenesis promotes tumour growth and is associated with a poorer prognosis [26]. However, the efficacy of radioembolization also depends on a preferential arterial vascularisation of liver tumours [27–29]. Therefore, ^{99m}Tc-MAA uptake could be both a negative prognostic biomarker and a positive predictive biomarker for treatment efficacy of radioembolization. The results of our univariate analysis showed that $TLR_{MAA} \geq 1.9$ was associated with prolonged OS though this was not statistically significant in multivariate analysis. However, the 1.9 cut-off used in this study has not been derived by a method to optimize the predictive power, such as receiver operating characteristic curve. These results suggest that the negative prognostic value of a high tumour vascularisation is more than compensated by the increased efficacy of radioembolization in such an environment, although this should be further elucidated in future trials.

Finally, the recently started Phase III SIRCCA trial (clinicaltrials.gov identifier NCT02807181) is currently recruiting patients with unresectable IH-CCA. This study is a prospective, multicenter, randomised, controlled study evaluating radioembolization with resin ^{90}Y-microspheres preceding standard cisplatin-gemcitabine chemotherapy versus cisplatin-gemcitabine chemotherapy alone as first-line treatment. Per protocol, the prescribed activity of ^{90}Y-microphores should be determined either using the BSA or the partition-model. In regard to the results of our study, the SIRCCA trial as well as future studies on radioembolization should stratify patients according to the method used to compute the activity of ^{90}Y-microsphere to administer in their analysis. Recently, a large randomised multicentre trial by Wasan et al. showed a non-benefit of the combination of radioembolization with FOLFOX in terms of PFS and OS [18–20]. The prescribed ^{90}Y-microsphere activity to administer was computed using an even more conservative variant of the standard BSA method, in which the activity prescription first linearly increases till tumour involvement of 50/55% and then decreases for very high tumor load (>50%), whereas in the classical BSA method (used in our study) this value increases linearly [11, 19]. Thus, tumour underdosage could mainly explain the absence of benefit.

This work reports the results of a European multicentre retrospective study on patients with unresectable IH-CCA, refractory to surgery and/or chemotherapy, treated with resin ^{90}Y-microspheres, and, to the best of our knowledge, the first to demonstrate clinically significant overall survival difference between patients treated according to the partition-model versus the widely-used BSA method. Our results support that partition-model should be prioritized in patients with unresectable and refractory IH-CCA treated with radioembolization. Other cancer types treated with radioembolization should be studied as they might also benefit from a more personalized activity prescription method.

Several limitations of this study should be noted. This is a multicenter study based on the data of four European radioembolization expert centres. The first limitation of our study is its retrospective character, and so the study is subject to bias. Data and images were not acquired in all patients because of differences in clinical practices between centres. Also, the small number of patients ($n = 58$) limits the application of our results in an external dataset, which is ineluctably due to the low incidence of IH-CCA patients in western countries. It is uncertain whether the results would be reproduced in non-expert centres for radioembolization. Finally, because of the high impact of the activity prescription method (partition-model vs BSA) on OS, the impact of clinical, biological and imaging biomarkers cannot be fully assessed in this relatively small cohort of patients. These biomarkers should still be evaluated in further trials and in patients stratified according to the activity prescription method. Prospective studies are required to validate our results.

Conclusion

In patients with unresectable and refractory IH-CCA treated with radioembolization, personalised radioembolization activity prescription using the partition model was associated with higher mean absorbed doses to tumour and consequently to an improved OS compared to the widely used BSA method.

Acknowledgments This academic work was supported and sponsored by the Jules Bordet Institute. Part of the results was presented at the 2019 SNMMI–annual congress of the Society of Nuclear Medicine and Molecular Imaging as an oral presentation during the GI – Colorectal, liver, esophageal session (OP- 216).

Funding This work was not supported by a grant.

Compliance with ethical standards

Conflict of interest PF, AH, HA and CD played an advisory role and received honoraria from Sirtex.

ML is a consultant for BTG, Sirtex, Quirem and Terumo. He receives research support from BTG, Quirem and Terumo. The department of Radiology and Nuclear Medicine of the UMC Utrecht receives royalties from Quirem.

BV played an advisory role and received honoraria from Dosisoft.

The first author and all other co-authors have no conflicts of interest to disclose.

Ethical approval All procedures performed in studies involving human participants were in accordance with the ethical standards of the institutional and/or national research committee and with the 1964 Helsinki declaration and its later amendments or comparable ethical standards. This study was approved by the Jules Bordet Institute Ethics Committee (CE2575) and Ethics Committees of all other participating centres. For this type of study formal consent is not required.

This article does not contain any studies with animals performed by any of the authors.

References

1. Khan SA, Toledano MB, Taylor-Robinson SD. Epidemiology, risk factors, and pathogenesis of cholangiocarcinoma. Hpb. 2008;10:77–82. Available from: http://linkinghub.elsevier.com/retrieve/pii/S1365182X1530023X. Accessed Apr 2008.
2. Cucchetti A, Cappelli A, Mosconi C, Zhong JH, Cescon M, Pinna AD, et al. Improving patient selection for selective internal radiation therapy of intra-hepatic cholangiocarcinoma: a meta-regression study. Liver Int. 2017;37:1056–64.
3. Park J, Kim MH, Kim KP, Park DH, Moon SH, Song TJ, et al. Natural history and prognostic factors of advanced cholangiocarcinoma without surgery, chemotherapy, or radiotherapy: a large-scale observational study. Gut Liver. 2009;3:298–305.
4. Tan JCC, Coburn NG, Baxter NN, Kiss A, Law CHL. Surgical management of intrahepatic cholangiocarcinoma—a population-based study. Ann Surg Oncol. 2008;15:600–8.
5. Currie B, Soulen M. Decision making: intra-arterial therapies for cholangiocarcinoma—TACE and TARE. Semin Intervent Radiol. 2017;34:092–100. https://doi.org/10.1055/s-0037-1602591.
6. Valle J, Wasan H, Palmer DH, Cunningham D, Anthoney A, Maraveyas A, et al. Cisplatin plus gemcitabine versus gemcitabine for biliary tract cancer. N Engl J Med. 2010;362:1273–81. https://doi.org/10.1056/NEJMoa0908721.
7. Rafi S, Piduru SM, El-Rayes B, Kauh JS, Kooby DA, Sarmiento JM, et al. Yttrium-90 radioembolization for unresectable standard-chemorefractory intrahepatic cholangiocarcinoma: survival, efficacy, and safety study. Cardiovasc Intervent Radiol. 2013;36:440–8.
8. Saxena A, Bester L, Chua TC, Chu FC, Morris DL. Yttrium-90 radiotherapy for unresectable intrahepatic cholangiocarcinoma: a preliminary assessment of this novel treatment option. Ann Surg Oncol. 2010;17:484–91. https://doi.org/10.1245/s10434-009-0777-x.
9. Hoffmann RT, Paprottka PM, Schön A, Bamberg F, Haug A, Dürr EM, et al. Transarterial hepatic yttrium-90 radioembolization in patients with unresectable intrahepatic cholangiocarcinoma: factors associated with prolonged survival. Cardiovasc Intervent Radiol. 2012;35:105–16.
10. Wahl RL, Jacene H, Kasamon Y, Lodge MA. From RECIST to PERCIST: evolving considerations for PET response criteria in solid tumors. J Nucl Med. 2009;50(Suppl 1):122S–50S. Available from: http://www.pubmedcentral.nih.gov/articlerender.fcgi?artid=2755245&tool=pmcentrez&rendertype=abstract. Accessed 1 Oct 2009.
11. Grosser OS, Ulrich G, Furth C, Pech M, Ricke J, Amthauer H, et al. Intrahepatic activity distribution in radioembolization with Yttrium-90–labeled resin microspheres using the body surface area method—a less than perfect model. J Vasc Interv Radiol. 2015;26(11):1615–21. Available from: https://www.sciencedirect.com/science/article/pii/S1051044315006995?via%3Dihub. Accessed 28 Aug 2015.
12. Ho S, Lau WY, Leung TWT, Chan M, Ngar YK, Johnson PJ, et al. Partition model for estimating radiation doses from yttrium-90 microspheres in treating hepatic tumours. Eur J Nucl Med. 1996;23:947–52.
13. Dieudonne A., Garin E, Laffont S, Rolland Y, Lebtahi R, Leguludec D, et al. Clinical feasibility of fast 3-dimensional dosimetry of the liver for treatment planning of hepatocellular carcinoma with 90Y-Microspheres. J Nucl Med 2011;52:1930–1937.
14. Levillain H, Duran Derijckere I, Marin G, Guiot T, Vouche M, Reynaert N, et al. 90Y-PET/CT-based dosimetry after selective internal radiation therapy predicts outcome in patients with liver metastases from colorectal cancer. EJNMMI Res. 2018;8:60. https://doi.org/10.1186/s13550-018-0419-z.
15. van den Hoven AF, Rosenbaum CENM, Elias SG, de Jong HWAM, Koopman M, Verkooijen HM, et al. Insights into the dose-response relationship of radioembolization with resin 90Y-Microspheres: a prospective cohort study in patients with colorectal cancer liver metastases. J Nucl Med. 2016;57:1014–9. https://doi.org/10.2967/jnumed.115.166942.
16. Willowson KP, Hayes AR, Chan DLH, Tapner M, Bernard EJ, Maher R, et al. Clinical and imaging-based prognostic factors in radioembolisation of liver metastases from colorectal cancer: a retrospective exploratory analysis. EJNMMI Res. 2017;7:46. https://doi.org/10.1186/s13550-017-0292-1.
17. Yttrium S-S. Resin microspheres [package insert]. North Sydney. Australia: SirTex Medical; 2017. Available from: https://www.sirtex.com/media/155126/ssl-us-13.pdf.
18. Wasan HS, Gibbs P, Sharma NK, Taieb J, Heinemann V, Ricke J, et al. First-line selective internal radiotherapy plus chemotherapy versus chemotherapy alone in patients with liver metastases from colorectal cancer (FOXFIRE, SIRFLOX, and FOXFIRE-global): a combined analysis of three multicentre, randomised, phase 3 trials. Lancet Oncol. 2017;18:1159–71.
19. Gibbs P, Gebski V, Van Buskirk M, Thurston K, Cade DN, Van Hazel GA, et al. Selective internal radiation therapy (SIRT) with yttrium-90 resin microspheres plus standard systemic chemotherapy regimen of FOLFOX versus FOLFOX alone as first-line treatment of non-resectable liver metastases from colorectal cancer: the SIRFLOX study. BMC Cancer. 2014;14:1–10.
20. Dutton SJ, Kenealy N, Love SB, Wasan HS, Sharma RA. FOXFIRE protocol: an open-label, randomised, phase III trial of 5-fluorouracil, oxaliplatin and folinic acid (OxMdG) with or without interventional selective internal radiation therapy (SIRT) as first-line treatment for patients with unresectable liver-on. BMC Cancer. 2014;14:497. Available from: http://onlinelibrary.wiley.com/o/cochrane/clcentral/articles/279/CN-01115279/frame.html. Accessed 31 Jan 2016.
21. Cremonesi M, Chiesa C, Strigari L, Ferrari M, Botta F, Guerriero F, et al. Radioembolization of hepatic lesions from a radiobiology and dosimetric perspective. Front Oncol. 2014;4:210.

22. Kao YH, Hock Tan AE, Burgmans MC, Irani FG, Khoo LS, Gong Lo RH, et al. Image-guided personalized predictive dosimetry by artery-specific SPECT/CT partition modeling for safe and effective 90Y Radioembolization. J Nucl Med 2012;53:559–566. Available from: http://www.ncbi.nlm.nih.gov/pubmed/22343503. Accessed 17 Sep 2012.
23. Woff E, Hendlisz A, Garcia C, Deleporte A, Delaunoit T, Maréchal R, et al. Monitoring metabolic response using FDG PET-CT during targeted therapy for metastatic colorectal cancer. Eur J Nucl Med Mol Imaging. 2016;43:1792–801. https://doi.org/10.1007/s00259-016-3365-x.
24. Zhu AX, Meyerhardt JA, Blaszkowsky LS, Kambadakone AR, Muzikansky A, Zheng H, et al. Efficacy and safety of gemcitabine, oxaliplatin, and bevacizumab in advanced biliary-tract cancers and correlation of changes in 18-fluorodeoxyglucose PET with clinical outcome: a phase 2 study. Lancet Oncol. 2010;11:48–54.
25. Haug AR, Heinemann V, Bruns CJ, Hoffmann R, Jakobs T, Bartenstein P, et al. 18F-FDG PET independently predicts survival in patients with cholangiocellular carcinoma treated with 90Y microspheres. Eur J Nucl Med Mol Imaging. 2011;38:1037–45.
26. Thelen A, Scholz A, Weichert W, Wiedenmann B, Neuhaus P, Gener R, et al. Tumor-associated angiogenesis and lymphangiogenesis correlate with progression of intrahepatic cholangiocarcinoma. Am J Gastroenterol. 2010;105:1123–32.
27. Flamen P, Vanderlinden B, Delatte P, Ghanem G, Ameye L, Van Den Eynde M, et al. Multimodality imaging can predict the metabolic response of unresectable colorectal liver metastases to radioembolization therapy with Yttrium-90 labeled resin microspheres. Phys Med Biol. 2008;53:6591–603.
28. Garin E, Lenoir L, Rolland Y, Edeline J, Mesbah H, Laffont S, et al. Dosimetry based on 99mTc-macroaggregated albumin SPECT/CT accurately predicts tumor response and survival in hepatocellular carcinoma patients treated with 90Y-loaded glass Microspheres: preliminary results. J Nucl Med. 2012;53:255–63. https://doi.org/10.2967/jnumed.111.094235.
29. Manceau V, Palard X, Rolland Y, Pracht M, Le Sourd S, Laffont S, et al. A MAA-based dosimetric study in patients with intrahepatic cholangiocarcinoma treated with a combination of chemotherapy and 90Y-loaded glass microsphere selective internal radiation therapy. Eur J Nucl Med Mol Imaging. 2018;45(10):1731–41. Available from: https://link.springer.com/article/10.1007%2Fs00259-018-3990-7. Accessed 20 Mar 2018.

Affiliations

Hugo Levillain[1] · Ivan Duran Derijckere[1] · Lieveke Ameye[2] · Thomas Guiot[3] · Arthur Braat[4] · Carsten Meyer[5] · Bruno Vanderlinden[3] · Nick Reynaert[3] · Alain Hendlisz[6] · Marnix Lam[4] · Christophe M. Deroose[7] · Hojjat Ahmadzadehfar[8] · Patrick Flamen[1]

1 Nuclear Medicine Department, Jules Bordet Institute, Université Libre de Bruxelles, 1 rue Héger-Bordet, 1000 Brussels, Belgium

2 Data Center Department, Jules Bordet Institute, Université Libre de Bruxelles, 1 rue Héger-Bordet, 1000 Brussels, Belgium

3 Medical Physics Department, Jules Bordet Institute, Université Libre de Bruxelles, 1 rue Héger-Bordet, 1000 Brussels, Belgium

4 Radiology and Nuclear Medicine Department, University Medical Center Utrecht, Heidelberglaan 100, 3584, CX Utrecht, The Netherlands

5 Radiology Department, University Hospital Bonn, Sigmund-Freud-Str. 25, 53127 Bonn, Germany

6 Digestive Oncology Department, Jules Bordet Institute, Université Libre de Bruxelles, 1 rue Héger-Bordet, 1000 Brussels, Belgium

7 Department of Imaging and Pathology, Nuclear Medicine, University Hospitals Leuven and Nuclear Medicine and Molecular Imaging, KU Leuven, Herestraat 49, 3000 Leuven, Belgium

8 Nuclear Medicine Department, University Hospital Bonn, Sigmund-Freud-Str. 25, 53127 Bonn, Germany